TransNav
http://www.transnav.eu
the International Journal on Marine Navigation and Safety of Sea Transportation
Volume 18
Number 4
December 2024
DOI: 10.12716/1001.18.04.17

Comparative Assessment of the Effect of Changing the Breadth (B) of the Ship on the Stability of the Tugboat

A. Alamsyah[1], M. Fikri[1], S. Suardi[1], M.U. Pawara[1], R.J. Ikhwani[1], W. Setiawan[1] & D. Paroka[2]
[1]*Institut Teknologi Kalimantan, Balikpapan, Indonesia*
[2]*Hasanuddin University, Gowa, South Sulawesi, Indonesia*

ABSTRACT: This paper reviews the effect of changing the breadth of a tugboat before and after production on ship stability. The numerical simulation method (maxurf stability) is applied. Likewise, another approach uses the Benjamin Spence (integrator) method. The standard used is IMO. Several limits become parameters for assessing the increase and decrease in ship stability. Several ship load cases are simulated to produce righting arm curves. The construction of a tugboat with a length of 28 meters is the object of this research as a case study. We compared the righting arm curve from the Maxurf stability analysis with Benjamin Spence's analysis to confirm the accuracy of the calculation results. Both methods show a significant influence regarding changes in the breadth of the tugboat. The produced righting arm curve consistently shows changes in the stability and performance of the ship. There is a reduction in the area under the GZ curve. The IMO provides three of the five standards and recommendations regarding the area under the GZ curve. The reduction of the area under the GZ curve is 17~22% for the Benjamin Spence method and 12~18% for the Maxurf stability. This percentage applies to all load-case simulations. This research contributes to providing an understanding of the effect of changes in ship width on decreasing stability.

1 INTRODUCTION

Sea transportation has a much greater risk of accidents than other means of transportation. Dynamic and unpredictable shipping conditions have implications for comfort [1]. The condition of the maritime industry is the same. Always with different challenges every time. One industry that is in line with this is the mining industry. This industry requires massive sea transportation to support the supply chain from upstream to downstream.

One of the identical modes of maritime industry is the tugboat. The construction of very massive tugboats usually uses certain methods, depending on the shipyard facilities [2][3]. Usually built in pairs with a deck barge, Used to tow deck barges containing mining products. Apart from that, it is also used as a pilot boat and for mooring activities on large ships in the port.

Much research has been done on tugboats [4][5] as well as on barges [6][7][8][9]. Considering that tugboats and barges are a mode of sea transportation that is used massively, this research study aims to optimize their operation to support maritime industry activities, especially the shipping sector.

Tugboats are required to have high performance in terms of maneuvering, stability, power, and maneuverability because of their habitat and function when operating. Ship maneuvering will be greatly influenced by the characteristics of the water depth [10]. The ship's maneuvering movements can be controlled with a virtual automatic identification system and camera data [11]. Likewise, powering will be greatly influenced by the ship's resistance when operating [12]. On the other hand, ship stability shows a significant influence from the even distribution of cargo weight [13]. Placing cargo positions on different decks will affect the stability of the ship [14].

Ship stability studies have been carried out using various methods and approaches. The type of ship is also a choice. Because it has its own characteristics based on the size and shipping area. Hyeon Kim et al. [15] studied the safety limits of submarine operations with stability aspects. Woo et al. [16] evaluate ship stability using a simple method based on cargo safety with approximately 20 load cases. Negi et al. [17] examine the steps for logically implementing second-generation intact stability (SGISC) to detect failure modes early [18]. Studies related to SGISC are very interesting and are being massively encouraged [19][20][21][22]. Guo et al. [23] studying the dynamic rolling behavior of ships using algorithms. Paroka et al. [24] Study the stability of traditional wooden ships using alternative methods and evaluate them using second-generation stability and weather criteria [25] and weather criteria [26]. The study focuses on comparing the breadth and draft of the ship's B/T against the applicable criteria [27]. These studies used an experimental test-method approach in experimental tanks.

The shape of the ship's hull affects the quality of the design, stability conditions, and other aspects of production [15][28][29][30]. Apart from that, the main size ratio also plays a role in determining the performance of the ship [27]. In this research, we also examine the main size ratios that have a significant effect on ship stability performance. Construction and design of a tugboat with a length of 28 meters as a case study object. The design breadth of the ship is B = 9 m, but during production the breadth was reduced to B = 8.6 meters with the design height and draft remaining the same. In terms of material use, it is relatively profitable because there is a reduction, but from a technical perspective and the performance of the ship, it will have a big impact, such as maneuverability, stability, powering, and maneuverability. The focus of this research is on how the ship's stability performance occurs after breadth reduction. Previous ship stability studies used samples of container ships, submarines, passenger ships, and traditional wooden ships. Likewise, the method used is an experimental test. In contrast to our research, which uses a tugboat case study with a numerical simulation method approach using maxurf stability [31][32][33] and the Benjamin Spence (integrator) method [34][35].

2 METHODOLOGY

2.1 *Benjamin Spence Method*

This method is often used. To determine the buoyancy value and metacentre point (Mo), Benjamin created several water lines (WL) parallel to the cross section of the ship [36][37].

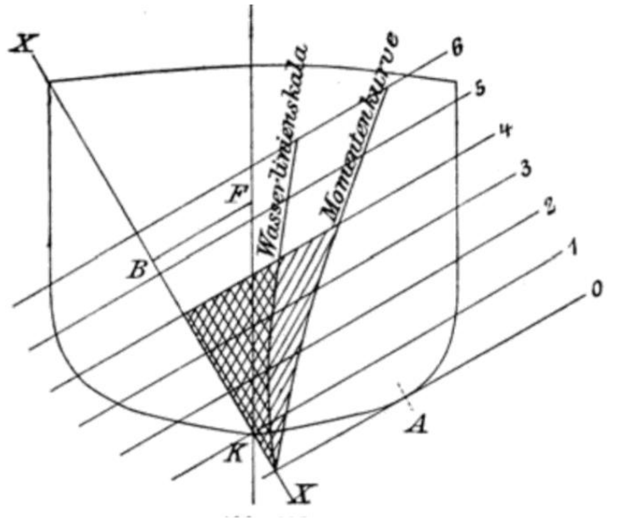

Figure 1. Parallel water lines of a ship's cross section

Figure 1 provides the coordinates for creating the cross-sectional area of the water line (A_{WL}) and the pressure point (T_{cf}), as well as the static moment. In the process, we use Simpson's First Rules. This condition is carried out repeatedly at every angle of inclination to produce pantocarena. The Panto Carena curve (cross curve) connects the arm value (NK sin φ) and the ship displacement value (Δ).

$$\Delta = \nabla \cdot \gamma \cdot c \tag{1}$$

$$\nabla = \frac{1}{3} \cdot h_{draft} \cdot \sum A_{WL} \cdot Fs \tag{2}$$

$$A_{WL} = \frac{1}{3} \cdot L_{station} \cdot \sum (ym + yk) \cdot Fs \tag{3}$$

$$T_{cf} = \frac{1}{2} \cdot \frac{\sum (ym - yk) \cdot (ym + yk) \cdot Fs}{\sum (ym + yk) \cdot Fs} \tag{4}$$

$$NK \sin \varphi = \frac{\sum A_{WL} \cdot Fs \cdot T_{cf}}{\sum A_{WL} \cdot Fs} \tag{5}$$

where Δ is displacement [tons]; γ is the density of sea water [1.025 tons/m^3]; c is the skin factor = 1.00675 – 1.0075 for steel ships; ∇ is volume [m^3]; h_{draft} is the distance between waterlines [meters]; A_{WL} is the cross-sectional area of the water line [m^2]; F_s is the Simpsons factor; $L_{station}$ is the distance between stations [meters]; ym is the horizontal distance of the KK axis (centre line) to the point where the water line intersects with the right hull section line [meters]; yk is the horizontal distance of the KK axis (centre line) to the point where the water line intersects with the left hull section line [meters]; -yk is a condition where the horizontal distance of the KK axis (center line) to the point where the waterline intersects with the left hull section line is not detected and follows the ym direction of the right hull [meters]; and T_{cf} is the pressure point of the water line measured from the KK (centerline) [meters].

The next step is to calculate the weight components and center of gravity of the ship.

$$\Delta_{weight} = \mathrm{LWT} + \mathrm{DWT} \tag{6}$$

$$KG = \frac{\sum \mathrm{M}}{\sum w} \tag{7}$$

where Δweight is the displacement weight [tons]; LWT is light weight tons [tons]; DWT is dead weight tons [tons]; KG is the total vertical gravity of the ship [meters]; for steel ships, ∇ is volume [m3]; Σw is total weight [tons]; and ΣM is the total force moment [tons.meters].

Next, calculate and draw the curve of the righting arm at each tilt angle. The righting arm (h) will be the parameter as required by IMO [18].

$$h = NK \sin\varphi - KG \sin\varphi \tag{8}$$

where h is the righting arm [meters]; NK sin φ is the buoyancy arm [meters]; and KG sin φ is the arm of gravity [meters].

2.2 *Numerical Simulation*

Construction and design of a tugboat with a length of 28 meters as a case study object. This ship was assembled at one of the yards in the IKN supporting area. The ship was modeled in 3D at a 1:1 scale using the Maxurf modeler and analyzed using Maxurf stability [31][32][33]. The hull form and main dimensions of the Tugboat are listed in Table 1, Table 2, and, for further visualization, Figure 1.

Table 1. Tugboat ship parameters B = 9.00

Descriptions		Unit	Value
Ship length	L	[m]	28.000
Ship breadth	B	[m]	9.000
Design ship draft	T	[m]	3.300
Ship depth	H	[m]	4.300
Frame spacing	a0	[m]	0.500
Volume	∇	[m^3]	335.480
Vertical Centre of Grafity	KG	[m]	3.370

Table 2. Tugboat ship parameters B = 8.60

Descriptions		Unit	Value
Ship length	L	[m]	28.000
Ship breadth	B	[m]	9.000
Design ship draft	T	[m]	3.300
Ship depth	H	[m]	4.300
Frame spacing	a0	[m]	0.500
Volume	∇	[m^3]	320.740
Vertical Centre of Grafity	KG	[m]	3.568

Figure 2 shows the main dimensions of the ship according to the initial design, with breadth (b) = 9.00 m, height (h) = 3.60 m, and length (lwl) = 25.8 m. The second stage is to design it in 2D, then develop it in 3D for ship breadth of 9.00 m and 8.60 m. The ship design is shown in Figure 3.

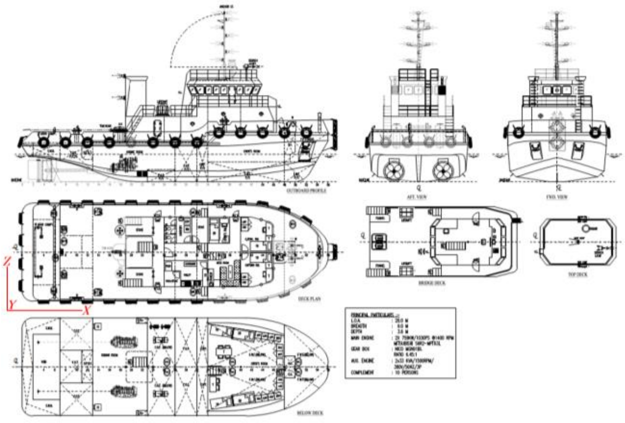

Figure 2. General Arragement

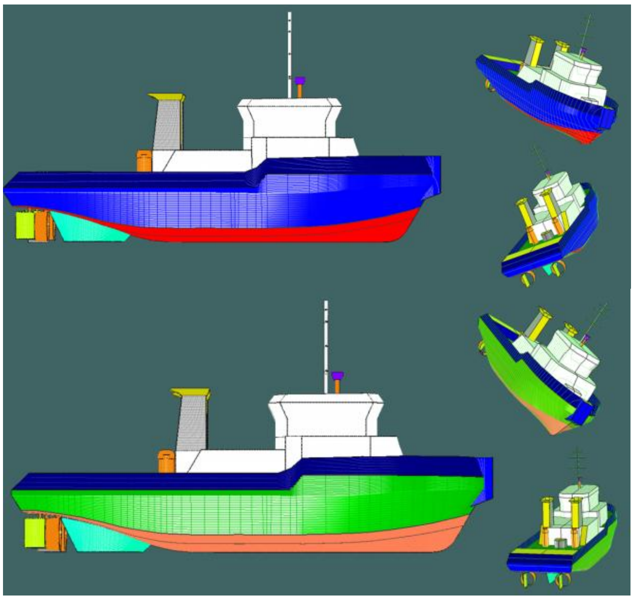

Figure 3. 3D ship with B=9.00 and B=8.60

The next stage is tank design. The tank dimensions seen in Figure 2 are developed in 3D form, as shown in Figure 4.

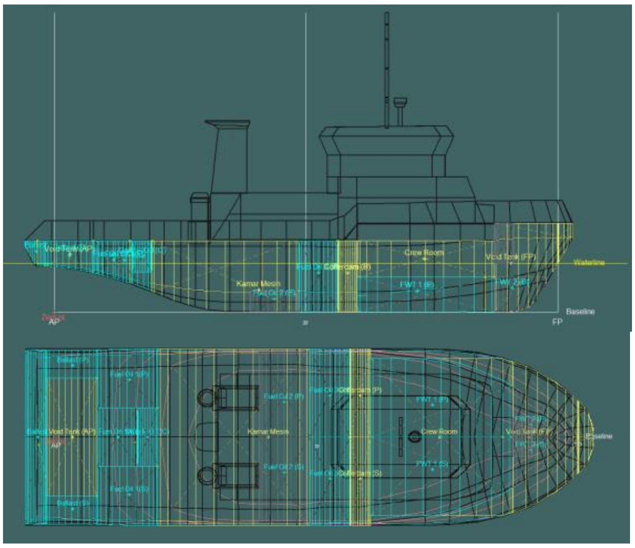

Figure 4. Ship tank modeling

The difference in ship breadth B = 9.00 m and B = 8.60 m results in changes in the ship's displacement, which is in line with changes in the ship's DWT and LWT, which can be seen below:

Table 3. Displacement of different

B of type	Δ [tons]	DWT [tons]	LWT [tons]	KG [m]
9.00	343.90	196.381	147.519	3.370
8.60	328.80	187.351	141.351	3.568

The next stage is a loadcase simulation by varying the ship's DWT by 100% DWT, 75% DWT, 50% DWT, and 25% DWT. Meanwhile, the LWT value adjusts to changes in the breadth of the ship.

Table 4. Laodcase tugboat B=9.00

Component	100% DWT [tons]	75% DWT [tons]	50% DWT [tons]	25% DWT [tons]
Lightship	147.51	147.51	147.51	147.51
Ballast tank	18.27	18.27	18.27	18.27
Dry fuel oil tank	4.019	4.019	4.019	4.019
Fuel oil tank	100.42	75.31	50.21	25.10
Fresh water tank	72.86	54.64	36.43	18.21

Table 5. Laodcase tugboat B=8.60

Component	100%			
Component	100% DWT [tons]	75% DWT [tons]	50% DWT [tons]	25% DWT [tons]
Lightship	141.35	141.35	141.35	141.35
Ballast tank	16.50	16.50	16.50	16.50
Dry fuel oil tank	4.019	4.019	4.019	4.019
Fuel oil tank	95.69	71.76	47.84	23.92
Fresh water tank	70.34	52.75	35.17	17.58

The loadcase set-up is applied to vessels B = 9.00 and B = 8.60. The goal is to find the righting arm curve. Next, it is evaluated based on IMO standards [18]. This work is to find out the recommended loadcase and vice versa when the ship is operating.

3 RESULT AND DISCUSSION

After the loadcase set-up is carried out, the righting arm curves for ships B=9.00 and B=8.60 are produced, which are shown in the following figure.

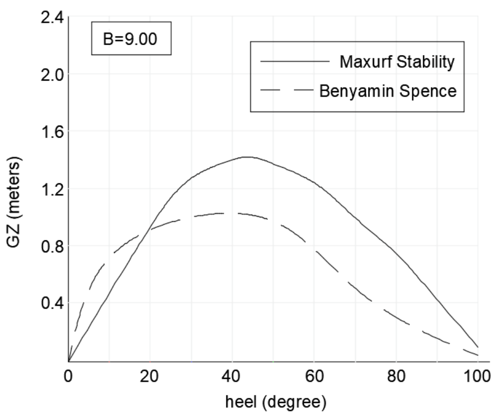

Figure 5. GZ curve B=9.00 of Loadcase 100%DWT

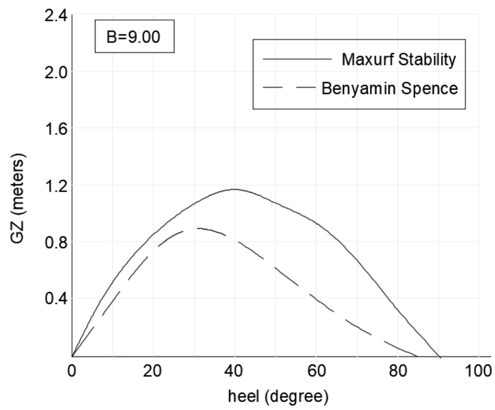

Figure 6. GZ curve B=9.00 of Loadcase 75%DWT

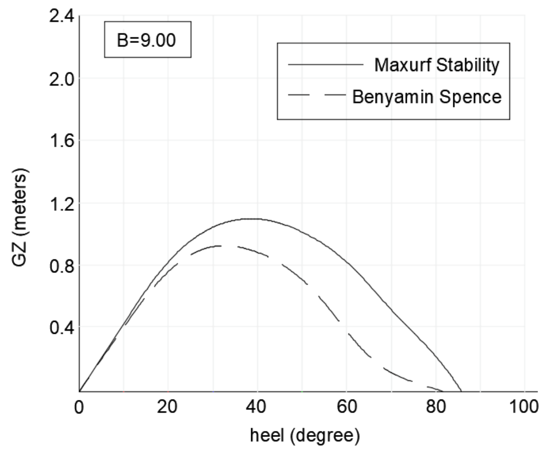

Figure 7. GZ curve B=9.00 of Loadcase 50%DWT

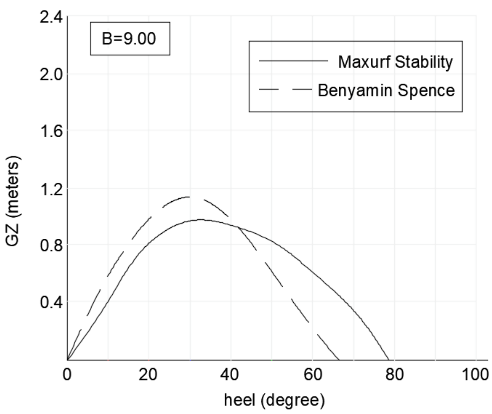

Figure 8. GZ curve B=9.00 of Loadcase 25%DWT

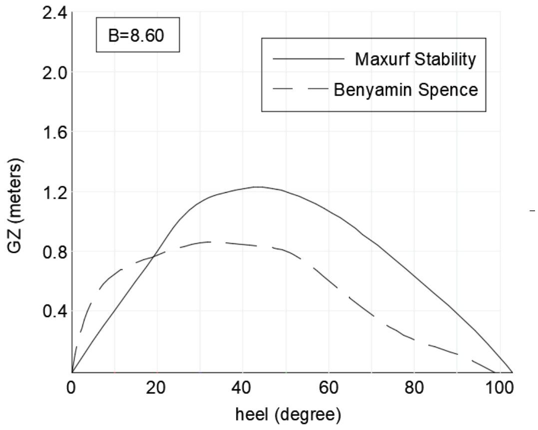

Figure 9. GZ curve B=8.60 of Loadcase 100%DWT

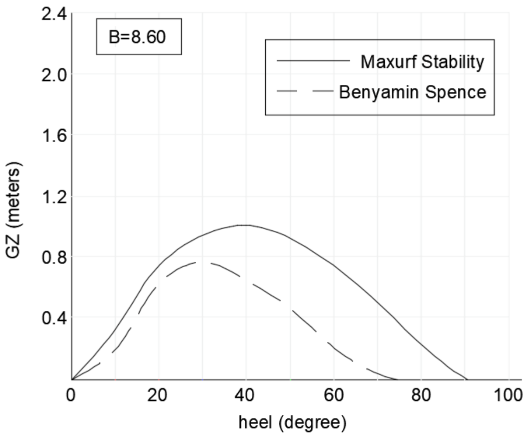

Figure 10. GZ curve B=8.60 of Loadcase 75%DWT

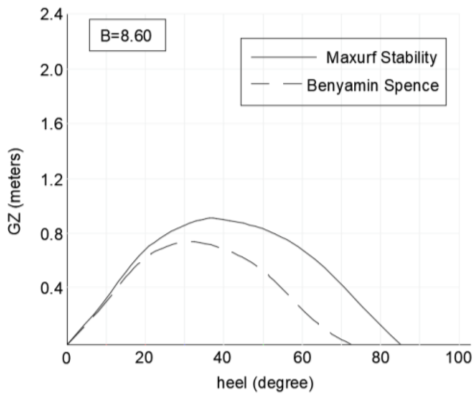

Figure 11. GZ curve B=8.60 of Loadcase 50%DWT

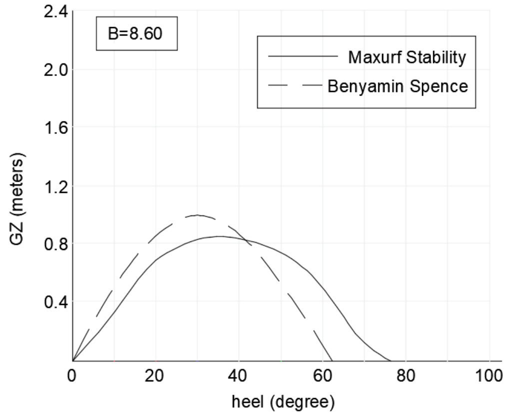

Figure 12. GZ curve B=8.60 of Loadcase 25%DWT

Figures 5 to 12 show the righting arm curves of ships with different breadths. More than one method is used to verify and validate calculation results. Also as a control for the results of the data analysis. The GZ curve is then summarized and evaluated based on IMO standards [18].

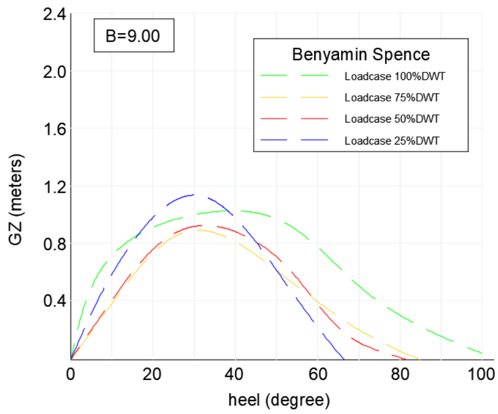

Figure 13. GZ curve B=9.00 of Loadcase all with Benyamin Spence

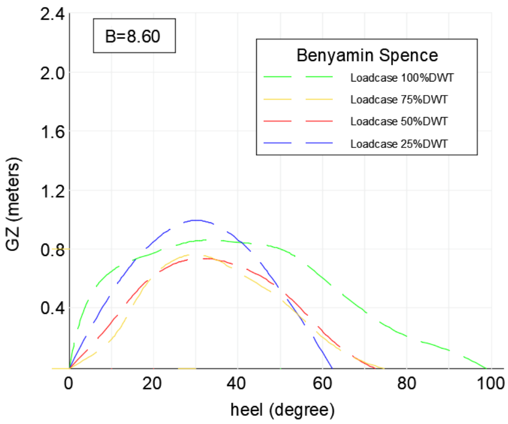

Figure 14. GZ curve B=8.60 of Loadcase all with Benyamin Spence.

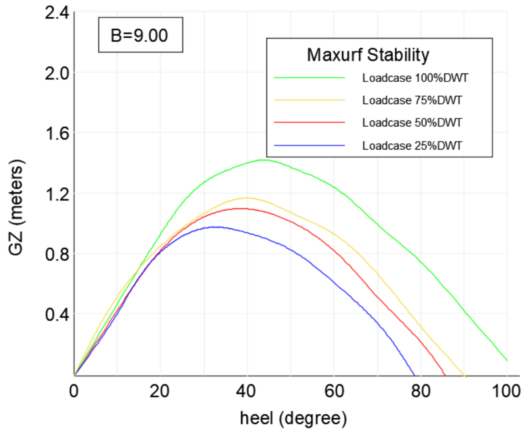

Figure 15. GZ curve B=9.00 of Loadcase all with Maxurf Stability.

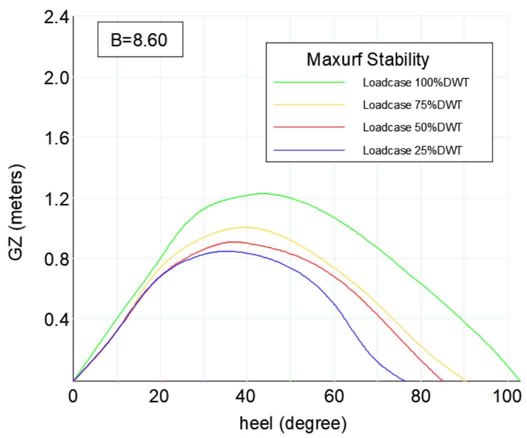

Figure 16. GZ curve B=9.00 of Loadcase all with Maxurf Stability.

Table 6. Evaluation of GZ curve B=9.00 from Maxurf Stability

Evaluation of Component	100% DWT	75% DWT	50% DWT	25% DWT
MG ⩾0.15 m	2.79	2.60	2.68	2.67
A0 – A30 ⩾3.151 m.deg	20.60	18.47	18.85	18.40
A0 – A40 ⩾5.156m.deg	34.13	29.99	31.01	28.20
A30 - A40 ⩾1.718m.deg	13.52	11.52	11.15	9.80
Max GZ at 30 or greater⩾0.2 m	1.41	1.17	1.13	0.98
Angle of maximum GZ⩾25 deg	42.70°	40°	38.2°	32.7°
Range of Stability > 60°	103°	90°	87°	75°

Table 7. Evaluation of GZ curve B=8.60 from Maxurf Stability

Evaluation of Component	100% DWT	75% DWT	50% DWT	25% DWT
MG ⩾0.15 m	2.39	2.20	2.26	2.23
A0 – A30 ⩾3.151 m.deg	17.83	18.47	15.81	15.11
A0 – A40 ⩾5.156m.deg	29.71	25.54	25.21	23.02
A30 - A40 ⩾1.718m.deg	11.88	9.88	9.40	7.90
Max GZ at 30 or greater⩾0.2 m	1.25	1.01	0.95	0.80
Angle of maximum GZ⩾25 deg	43.60°	40°	37.3°	31.8°
Range of Stability > 60°	102°	87°	82°	75°

Table 8. Evaluation of GZ curve B=9.00 from Benyamin Spence

Evaluation of Component	100% DWT	75% DWT	50% DWT	25% DWT
MG ⩾0.15 m	2.80	3.00	3.35	3.40
A0 – A30 ⩾3.151 m.deg	17.51	14.77	13.74	20.24
A0 – A40 ⩾5.156m.deg	20.47	16.49	21.08	29.61
A30 - A40 ⩾1.718m.deg	9.83	5.9	7.69	8.82
Max GZ at 30 or greater⩾0.2 m	1.05	0.87	0.85	1.15
Angle of maximum GZ⩾25 deg	40°	31°	32°	30°
Range of Stability > 60°	100.5°	84°	81.5°	66.5°

Table 9. Evaluation of GZ curve B=8.60 from Benyamin Spence

Evaluation of Component	100% DWT	75% DWT	50% DWT	25% DWT
MG ⩾0.15 m	2.73	2.90	3.20	3.31
A0 – A30 ⩾3.151 m.deg	17.80	14.77	13.43	16.61
A0 – A40 ⩾5.156m.deg	28.22	22.70	22.68	24.17
A30 - A40 ⩾1.718m.deg	6.53	6.91	6.48	8.29
Max GZ at 30 or greater⩾0.2 m	0.85	0.76	0.75	1.00
Angle of maximum GZ⩾25 deg	34°	30°	31°	30.5°
Range of Stability > 60°	98°	74.5°	71.9°	62°

Tables 6 to 9 show the evaluation of the GZ curve based on IMO standards. A ship with B = 9.00 shows superior stability compared to a ship with B = 8.60, even though both still meet the standard. There was a significant reduction in the area under the GZ curve, as shown in Figures 17 to 24. This can be seen in the GZ curve produced using the Benjamin Spence method and also in Maxurf stability.

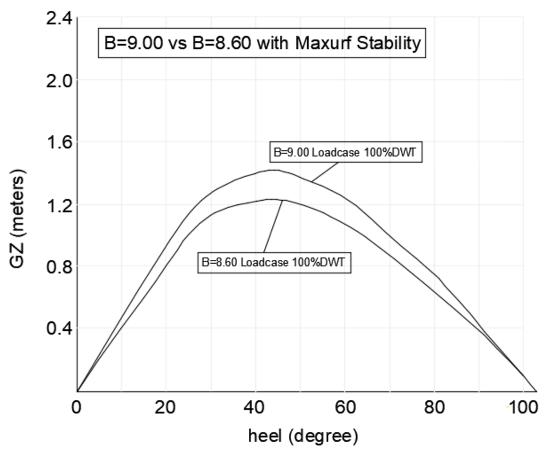

Figure 17. GZ curve B=9.00 vs B=8.60 of Loadcase 100%DWT with Maxurf Stability.

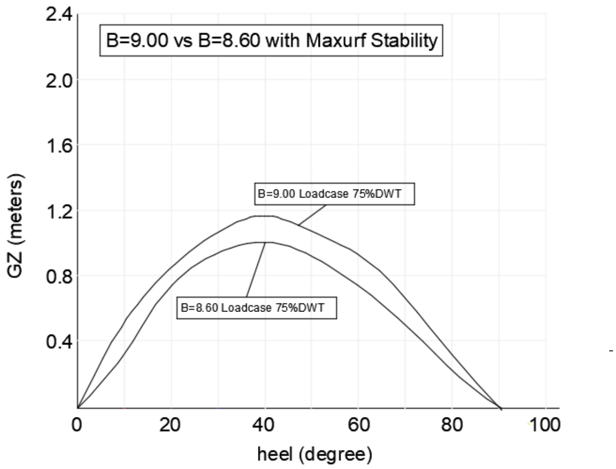

Figure 18. GZ curve B=9.00 vs B=8.60 of Loadcase 75%DWT with Maxurf Stability.

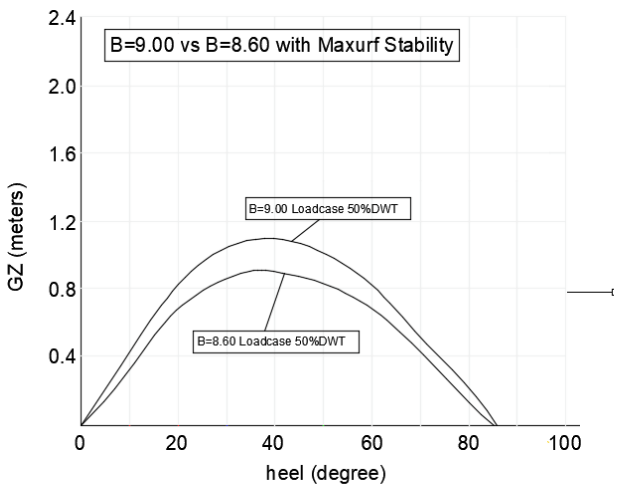

Figure 19. GZ curve B=9.00 vs B=8.60 of Loadcase 50%DWT with Maxurf Stability.

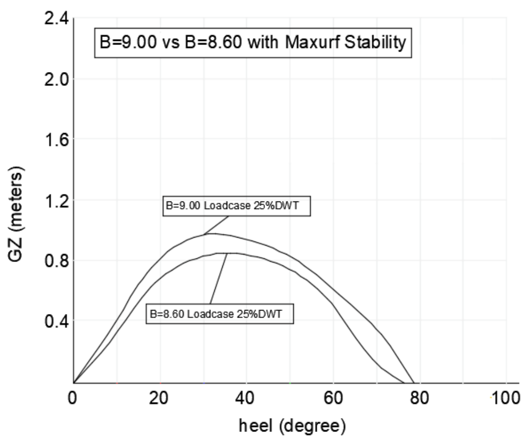

Figure 20. GZ curve B=9.00 vs B=8.60 of Loadcase 25%DWT with Maxurf Stability.

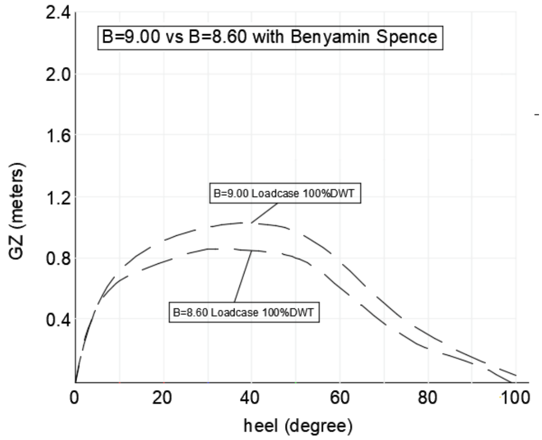

Figure 21. GZ curve B=9.00 vs B=8.60 of Loadcase 100%DWT with Benyamin Spence.

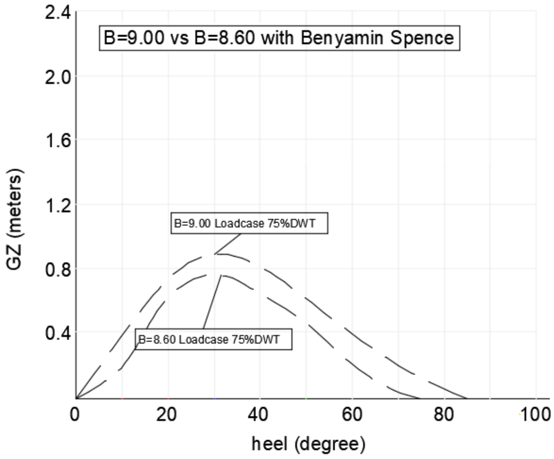

Figure 22. GZ curve B=9.00 vs B=8.60 of Loadcase 75%DWT with Benyamin Spence.

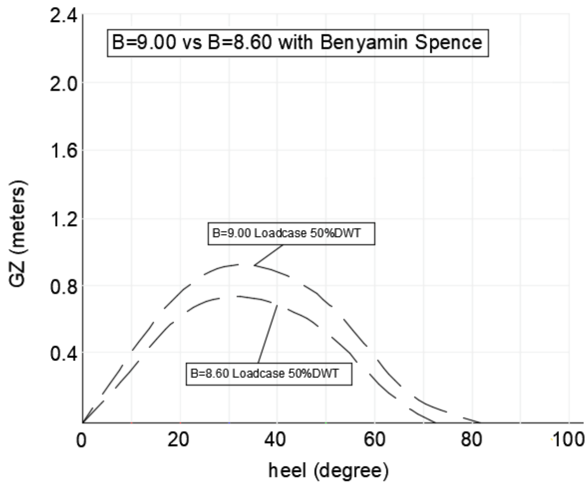

Figure 23. GZ curve B=9.00 vs B=8.60 of Loadcase 50%DWT with Benyamin Spence.

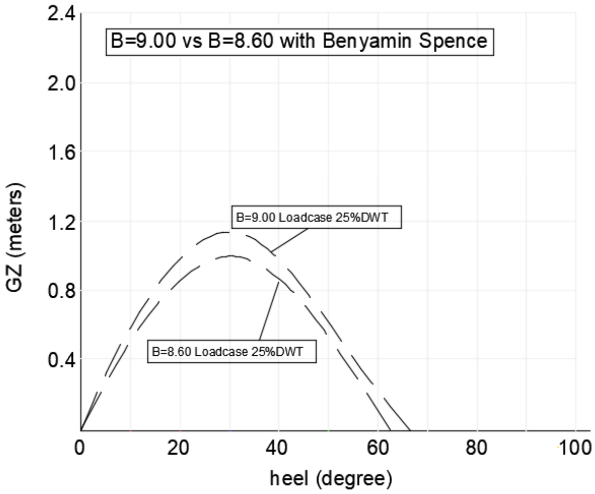

Figure 24. GZ curve B=9.00 vs B=8.60 of Loadcase 25%DWT with Benyamin Spence.

Figures 17 to 24 show a comparison of the GZ curve using the Benjamin Spence and Maxurf stability methods. The curve shows all loadcases before and after changing the breadth of the ship. Observations were made on the percentage reduction in area under the GZ curve. Benjamin Spence's method shows a reduction in the area under the GZ curve of 17 ~ 22%. Meanwhile, maxurf stability shows a reduction in the range of 12 to 18%.

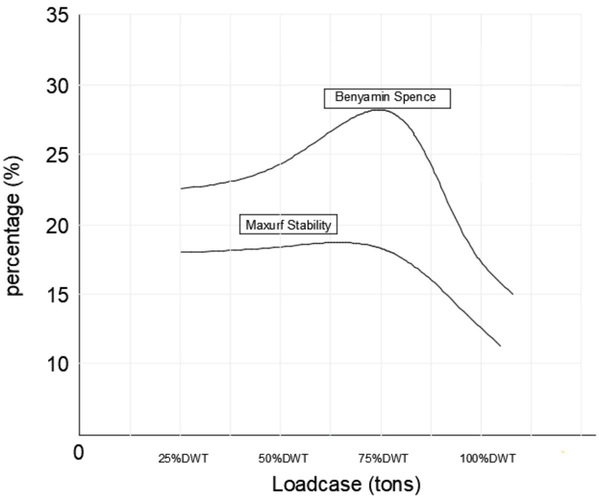

Figure 25. Percentage of reduce area under GZ curve maxurf stability vs benyamin spence.

Reducing the area under the GZ curve will have implications for stability and performance. After being evaluated based on IMO, the change in the breadth of the ship shows that it still meets the standards. However, changing the planning breadth and breadth during production is not recommended considering that tugboats have complex and dynamic habits, so they must have high stability like fishing boats, which require higher stability. [38][39][40][41][42][43][44][45][46].

4 CONCLUSIONS

This research, with data analysis, proves the significant influence related to changes in the breadth of tugboats. The Benjamin Spence and Maxurf stability methods consistently show changes in ship stability performance after changes in breadth. There is a reduction in the area under the GZ curve. The IMO provides three of five standards and recommendations regarding the area under the GZ curve. The reduction in area under the GZ curve is 17~22% for the Benjamin Spence method and 12~18% for Maxurf stability. This percentage applies to all load-case simulations. The next investigation will focus on stability analysis using other methods such as CFD, the ship shape coefficient approach, and, if necessary, experimental methods in experimental pools. Considering that tugboats have complex and dynamic habits, maneuvers, obstacles, and capsize opportunities will be investigated.

ACKNOWLEDGMENT

I acknowledge the support of time and facilities form Center of maritime infrastructure Engineering Kalimantan Institute of Technology University.

REFERENCES

[1] Langxiong Gan, L., et al., "Ship path planning based on safety potential field in inland rivers," Ocean Eng., vol. 260, no. 111928, pp. 1–9, 2022, [Online]. Available: https://www.sciencedirect.com/science/article/abs/pii/S0029801822012665.

[2] Rui Li, W.H., et al., "Development of multi-functional integrated design system for ship block lifting process," Int. J. Nav. Archit. Ocean Eng., vol. 16, no. 100593, pp. 1–11, 2024, [Online]. Available: https://pdf.sciencedirectassets.com/314106/1-s2.0-S2092678223X00028/1-s2.0-S2092678224000128/main.pdf?X-Amz-Security-Token=IQoJb3JpZ2luX2VjELb%2F%2F%2F%2F%2F%2F%2F%2F%2F%2FwEaCXVzLWVhc3QtMSJHMEUCIQCg%2BE9%2FYRGuF0Oh8FRV0xtHq4wHNvOfksybX9a0VBzEOAIgLEhxpbRW.

[3] Aguiari, M., M. Gaiotti, and C. M. Rizzo. "Ship weight reduction by parametric design of hull scantling," Ocean Eng., vol. 263, no. 112370, pp. 1–15, 2022, [Online]. Available: https://www.sciencedirect.com/science/article/abs/pii/S0029801822016626.

[4] Wang, L., et al., "Ship docking and undocking control with adaptive-mutation beetle swarm prediction algorithm," Ocean Eng., vol. 251, no. 111021, pp. 1–22, 2022, [Online]. Available: https://www.sciencedirect.com/science/article/abs/pii/S0029801822004425.

[5] Alamsyah, C. S. Kala, and A. I. Wulandari, "The Analysis of Engine Room Vibration of Tugboat 24 M," Marit. Park J. Marit. Technol. Soc., vol. 1, no. 3, pp. 93–101, 2022, [Online]. Available: https://journal.unhas.ac.id/index.php/maritimepark/article/view/23608.

[6] Hu, H., et al., "Study on the flooding characteristics of damaged barges with dynamic explosive deformation," Int. J. Nav. Archit. Ocean Eng., vol. 16, no. 100589, pp. 1–15, 2024, [Online]. Available: https://www.sciencedirect.com/science/article/pii/S2092678224000086.

[7] Alamsyah, et al., "The Fatigue Life Assessment of Sideboard on Deck Barge Using Finite Element Methods," J. Ind. Res. an Innov., vol. 16, no. 1, pp. 1–10, 2022, [Online]. Available: https://ejournal.brin.go.id/MIPI/article/view/1292.

[8] Alamsyah, et al., "Numerical Investigation of the Laying of Airbag Arrangements on Launching Barges," Int. J. Mar. Eng. Innov. Res., vol. 8, no. 2, pp. 202–212, 2023, [Online]. Available: https://iptek.its.ac.id/index.php/ijmeir/article/view/16737.

[9] Alamsyah, et al., "An Analyze of Fatigue Life Construction of Lifting Poonton for Small Vessel," Adv. Sci. Technol., vol. 104, pp. 95–101, 2021, [Online]. Available: https://www.scientific.net/AST.104.95.

[10] Nguyen, T.T., et al., "4DOF Maneuvering Motion of a Container Ship in Shallow Water Based on CFD Approach," Preprints.org, pp. 1–18, 2024, doi: doi:10.20944/preprints202404.1368.v1.

[11] Kong, M.C., and M. I. Roh, "A Method for Implementing a Ship Navigation Simulator for the Generation and Utilization of Virtual Data," Int. J. Nav. Archit. Ocean Eng., no. 100604, 2024, [Online]. Available: https://www.sciencedirect.com/science/article/pii/S2092678224000232?ref=pdf_download&fr=RR-2&rr=89ccd6adea955f5f.

[12] Baso, S., et al., "Experimental Investigation of Added Resistance of a Ship using a Hydroelastic Body in Waves," Int. J. Technol., vol. 13, no. 2, pp. 332–344, 2022, [Online]. Available: https://ijtech.eng.ui.ac.id/article/view/4904.

[13] Paroka, D., A. H. Muhammad, and S. Rahman, "Safety of an Indonesian ro-ro ferry with different weight distribution on vehicle deck," 2022, [Online]. Available: https://pubs.aip.org/aip/acp/article-abstract/2543/1/080009/2828934/Safety-of-an-Indonesian-ro-ro-ferry-with-different.

[14] Alamsyah, Z. Zulkarnaen, and Suardi, "The Stability Analyze of KM. Rejeki Baru Kharisma of Tarakan–Tanjung Selor Route," TEKNIK, vol. 42, no. 1, pp. 52–62, 2021, [Online]. Available: https://ejournal.undip.ac.id/index.php/teknik/article/view/31283;

[15] Kim, J.H., et al., "Limit Protection Systems for Safety Operational Envelope of Submarine," Int. J. Nav. Archit. Ocean Eng., no. 100598, 2024, [Online]. Available: https://www.sciencedirect.com/science/article/pii/S2092678224000177.

[16] Woo, D., and N. K. Im, "A Methodology for Simply Evaluating the Safety of a Passenger Ship Stability Using the Index for the Intact Stability Appraisal Module," Sensors, no. 1938, pp. 1–15, 2022, [Online]. Available: https://www.mdpi.com/1424-8220/22/5/1938.

[17] Negi, A., S. Ganesan T., and A. Ajithkumar, "On Prepration Of Operation Measures Under The Second Generation Of Intact Stability Criteria," 2023, [Online]. Available: https://www.researchgate.net/publication/377334701_ON_PREPRATION_OF_OPERATION_MEASURES_UNDER_THE_SECOND_GENERATION_OF_INTACT_STABILITY_CRITERIA.

[18] IMO MSC.1/Circ.1627, Interim Guidelines on the Second Generation Intact Stability Criteria. London, 2020.

[19] Petacco, N., G. Petkovic, and P. Gualeni, "An insight on the post-processing procedure of the Direct Stability Assessment within SGISC," Ocean Eng., vol. 305, no. 117982, pp. 1–14, 2024, [Online]. Available: https://www.sciencedirect.com/science/article/abs/pii/S0029801819303257.

[20] Bulian, G., and A. Francescutto, "Level 1 vulnerability criterion for the dead ship condition: A practical methodology for embedding operational limitations," Ocean Eng., vol. 272, no. 113868, pp. 1–12, 2023, [Online]. Available: https://www.sciencedirect.com/science/article/pii/S0029801823002524.

[21] Begović, E., et al., "Simplified operational guidance for second generation intact stability criteria," Ocean Eng., vol. 270, no. 113583, 2023, [Online]. Available: https://www.sciencedirect.com/science/article/abs/pii/S0029801822028669.

[22] Negi, A., and S. Ganesan T., "Assessment of Pure Loss of Stability Failure Mode for 2nd Generation Intact Stability," 2019.

[23] Guo, Z., et al., "Research on safety evaluation and weather routing optimization of ship based on roll dynamics and improved A* algorithm," Int. J. Nav. Archit. Ocean Eng., no. 100605, 2024, doi: https://doi.org/10.1016/j.ijnaoe.2024.100605.

[24] Paroka, D., et al., "Alternative Method for Stability Assessment of Indonesian Traditional Wooden Boats," in IOP Conference Series: Earth and Environmental Science, 2022, p. 012020, [Online]. Available: https://iopscience.iop.org/article/10.1088/1755-1315/972/1/012020/meta.

[25] Paroka, D., et al., "Operational limitation of Indonesian traditional wooden boat in the framework of second generation intact stability criteria," in IOP Conference Series: Earth and Environmental Science, 2021, p. 012064, [Online]. Available: https://iopscience.iop.org/article/10.1088/1755-1315/649/1/012064/meta.

[26] Asis, M.A., et al., "Experimental Study on Weather Criterion Applied to South Sulawesi Traditional Wooden Boats," in The 5th International Conference on Marine Technology (SENTA 2020), 2021, pp. 1–11.

[27] Paroka, D., et al., "Vulnerability of Ship with a Large Breadth to Draught Ratio Against Excessive Acceleration Criteria," in IOP Conference Series: Earth and Environmental Science, 2023, p. 012008, [Online]. Available: https://iopscience.iop.org/article/10.1088/1755-1315/1166/1/012008/meta.

[28] Alamsyah, et al., "Design of Fishing Vessel of Catamaran Type In Waterways of East Kalimantan (40 GT)," in Journal of Physics: Conference Series, 2021, p. 012014, [Online]. Available: https://iopscience.iop.org/article/ 10.1088/1742-6596/1726/1/012014/meta.

[29] Pawara, M.U., et al., "Bilge System Design on 500 GT Ferry for Bulukumba–Selayar Route," in IOP Conference Series: Earth and Environmental Science, 2021, p. 012010, [Online]. Available: https://iopscience.iop.org/article/10.1088/1755-1315/921/1/012010/meta.

[30] Alamsyah, et al., "Stability Study of Water Ambulance in East Kalimantan Inland Waterways," Wave J. Ilm. Teknol. Marit., vol. 17, no. 1, pp. 1–10, 2023, [Online]. Available: https://ejournal.brin.go.id/jurnalwave/article/view/186.

[31] Younis, G., et al., "Sensitivity Analyses of Intact and Damage Stability Properties to Passenger Ship's Dimensions and Proportions," PORT-SAID Eng. Res. J., vol. 23, no. 1, pp. 65–73, 2019, [Online]. Available: https://www.semanticscholar.org/paper/Sensitivity-Analyses-of-Intact-and-Damage-Stability-Younis-Abdelghany/65f404927affe95b1be199be570381d9235db283.

[32] Guan, G., et al., "Automatic optimal design of self-righting deck of USV based on combined optimization strategy," Ocean Eng., vol. 217, no. 107824, 2020, [Online]. Available: https://www.sciencedirect.com/science/article/abs/pii/S0029801820307988.

[33] Anggara, S., et al., "The Application of 2nd Generation Intact Stability Criteria to Ship Operating in Indonesia Waterway: Pureloss Stability," in IOP Conf. Series: Materials Science and Engineering, 2021, p. 1052, [Online]. Available: https://iopscience.iop.org/article/10.1088/1757-899X/1052/1/012050/pdf.

[34] Benjamin, L., Contributions to the solution of the problem of stability. Tr. of Inst. Nav. Arch, 1884.
[35] Spence, J.C., The Graphic calculation of the data depending on the form of ships, required for determining their stability. Tr. of Inst. Nav. Arch, 1884.
[36] Band, E., edited by E. Foerster, Hilfsbuch für den Schiffbau. 1928.
[37] Dudebout, P.e., "Stability of Ship," in Architecture navale : théorie du navire : I, 1890, p. 123.
[38] Yılmaz, H., and A. Kükner "Evaluation of cross curves of fishing vessels at the preliminary design stage," Ocean Eng., vol. 26, no. 10, pp. 979–990, 1999, [Online]. Available: https://www.sciencedirect.com/science/article/abs/pii/S0029801898000389.
[39] González, M.M., et al., "Fishing vessel stability assessment system," Ocean Eng., vol. 41, no. Februari, pp. 67–78, 2012, [Online]. Available: https://www.sciencedirect.com/science/article/abs/pii/S0029801811002988.
[40] Mantari, J.L., S.R.e. Silva, and G.C. Soares "Intact stability of fishing vessels under combined action of fishing gear, beam waves and wind," Ocean Eng., vol. 38, no. 17–18, pp. 1989–1999, 2011, [Online]. Available: https://www.sciencedirect.com/science/article/abs/pii/S0029801811002125.
[41] Masamoto, S., et al., "Experimental study of the water on deck effects on the transverse stability of a fishing vessel running in stern quartering seas," Ocean Eng., vol. 289, no. 116289, 2023, [Online]. Available: https://www.sciencedirect.com/science/article/abs/pii/S0029801823026732.
[42] Szozda, Z., and P. Krata, "Towards evaluation of the second generation intact stability criteria - Examination of a fishing vessel vulnerability to surf-riding, based on historical capsizing," Ocean Eng., vol. 248, no. 110796, 2022, [Online]. Available: https://www.sciencedirect.com/science/article/abs/pii/S0029801822002426.
[43] Santullano, F.M.A., and A.S. Iglesias, "Stability, safety and operability of small fishing vessels," Ocean Eng., vol. 79, no. March, pp. 81–91, 2014, [Online]. Available: https://www.sciencedirect.com/science/article/abs/pii/S0029801814000201.
[44] Caamaño, L.S., M. M. González, and V.D. Casas, "On the feasibility of a real time stability assessment for fishing vessels," Ocean Eng., vol. 159, no. July, pp. 76–87, 2018, [Online]. Available: https://www.sciencedirect.com/science/article/abs/pii/S0029801818304141.
[45] Caamaño, L.S., et al., "Evaluation of onboard stability assessment techniques under real operational conditions," Ocean Eng., vol. 258, no. 111841, 2022, [Online]. Available: https://www.sciencedirect.com/science/article/pii/S0029801822011842.
[46] Davis, B., B. Colbourne, and D. Molyneux, "Analysis of fishing vessel capsizing causes and links to operator stability training," Saferty Sci., vol. 118, no. October, pp. 355–363, 2019, [Online]. Available: https://www.sciencedirect.com/science/article/abs/pii/S0925753519300165.